Potassium Transport in *Neurospora*

Evidence for a multisite carrier at high pH

CAROLYN W. SLAYMAN and CLIFFORD L. SLAYMAN

From the Departments of Microbiology and Physiology, Yale University School of Medicine, New Haven, Connecticut 06510

ABSTRACT At low extracellular pH (4–6), net uptake of potassium by *Neurospora* is a simple exponential process which obeys Michaelis kinetics as a function of $[K]_o$. At high pH, however, potassium uptake becomes considerably more complex, and can be resolved into two distinct exponential components. The fast component (time constant = 1.2 min) is matched quantitatively by a rapid loss of sodium; it is attributed to ion exchange within the cell wall, since it is comparatively insensitive to low temperature and metabolic inhibitors. By contrast, the slower component (time constant = 10.9 min) is inhibited markedly at 0°C and by CN and deoxycorticosterone, and is thought to represent carrier-mediated transport of potassium across the cell membrane. This transport process exhibits sigmoid kinetics as a function of $[K]_o$; the data can be fitted satisfactorily by two different two-site models (one involving a carrier site and a modifier site, the other an allosteric model). Either of these models could also accommodate the simple Michaelis kinetics at low pH.

INTRODUCTION

The potassium content of the fungus *Neurospora* is regulated by a system that can transport a variety of monovalent cations across the cell membrane. Potassium influx, accompanied either by the efflux of sodium and hydrogen ions during net transport, or by efflux of potassium ions during steady-state exchange, is an energy-dependent, saturable function of the external potassium concentration. The same maximal influx, 20–23 mmoles/kg cell water · min, is observed during both K/K exchange and Na,H/K exchange, but the apparent Michaelis constants for external potassium are quite different in the two cases: 1.0 mM during K/K exchange, and 11.8 mM during Na,H/K exchange (40, 42). If a single system in the membrane is responsible for all three exchange processes, as seems likely from studies on transport mutants, then its apparent affinity for extracellular potassium is influenced by the nature of the exciting cation. Preliminary evidence has also suggested that ions other than those whose fluxes have been measured directly may react with the potassium

transport system. Extracellular ammonium,[1] rubidium, and sodium ions competively inhibit potassium influx (42), and choline, tris(hydroxymethyl)aminomethane[Tris], triethylamine, ethanolamine, and other amino cations produce rapid but reversible losses of sodium and potassium from *Neurospora* (40).

The reactions of hydrogen ions with the potassium pump are of special interest, even though the K pump is probably not the major route for hydrogen ion efflux. Base line, steady-state hydrogen ion efflux can amount to as much as 40 mmoles/kg cell water·min.[1] During net uptake of potassium at pH 5.8, there is an additional outward movement of hydrogen ions superimposed on the base line rate, with an initial velocity of 6–9 mmoles/kg cell water·min (roughly 30% of the maximal potassium influx). This takes place from an apparent intracellular H^+ concentration near 3×10^{-7} M, several orders of magnitude lower than the concentrations from which sodium and potassium are pumped, outward or inward. Net H^+ efflux ceases with rising intracellular potassium, perhaps because of competitive inhibition by potassium.

Whether extracellular hydrogen ions, as well as intracellular hydrogen, also react with the potassium pump has not previously been explored in *Neurospora*. The possibility is raised by observations on algae (38), bacteria (17), and yeast (1, 7), in which lowered extracellular pH leads to a decrease in potassium influx and a fall in the steady-state level of internal potassium. For yeast, on which the most extensive studies have been made, external hydrogen ions competitively inhibit potassium uptake in a manner which suggests that the potassium pump has a higher affinity (but only 3- to 15-fold) for hydrogen ions than for potassium ions (1). Recently, a noncompetitive "modifier" effect of hydrogen ions has also been postulated in yeast to account for the fact that the maximal velocity of potassium uptake is depressed at low external pH (2).

In order to determine whether extracellular hydrogen ions do in fact react with the potassium transport system in *Neurospora*, and whether a model similar to that developed for yeast is applicable, we have studied the effect of extracellular pH—in the range 3.5 to 9.0—on the rate and extent of net potassium uptake and sodium loss by low K, high Na cells of *Neurospora*.

METHODS

General The methods for growing low K *Neurospora*, carrying out the flux experiments, and analyzing the data are the same as those described previously (40). Wild-type strain RL21a of *Neurospora crassa* was used throughout the experiments. Conidia were inoculated at a density of 10^6/ml into shaking liquid cultures, 25°C, pH 5.8, with a medium initially containing 0.2 mM KCl. After 16 hr, the cells were har-

[1] Unpublished observations.

vested, rinsed several times in distilled water, and resuspended in K-free buffer solution, for a 20-min preincubation (25°C, continuous shaking). Potassium chloride was then added to the suspension in a small volume of 1 N solution, and 10 ml samples were harvested at intervals onto Millipore filters. Fluxes were stopped by three quick rinses with 10 ml distilled water. The cell mats, dried overnight at 90°C, were weighed and extracted in 1 N HCl at 100°C for 1 hr; flame analyses for sodium and potassium were carried out on these extracts.

The principal results, therefore, were obtained in units of micromoles K or Na per gram dry weight, which can be converted into apparent concentration units with the factor, intracellular water/dry weight = 2.54 (reference 41). Net fluxes were calculated from semilog plots of the data against time (0–30 min), using least squares estimates of slopes and intercepts. These fluxes can be converted into units of pmoles/$cm^2 \cdot sec$, with the relationship 1 mmole/kg cell water·min = 0.66 pmole/$cm^2 \cdot sec$. The derivation of this and the previous factor, along with considerations of their degree of accuracy, have been discussed previously (41, 42). Results throughout the paper are stated as mean ± 1 SE.

In the present experiments at pH 8 and above, as opposed to those carried out at pH 6 or below, a significant quantity of sodium and/or potassium ions appears bound to extracellular sites, presumably in the *Neurospora* cell wall (see p. 766). In order to avoid ambiguity in the text, we have adopted the following terminology and units: (*a*) "Cell wall potassium (or sodium)," in micromoles per gram dry weight; this component is also referred to as the "bound component" or, for fluxes, the "fast component." (*b*) "Intracellular potassium (or sodium)," usually in millimoles per kilogram cell water; also referred to as the "slow component" for fluxes. (*c*) "Total cell potassium (or sodium)," in micromoles per gram dry weight; this is the sum of (*a*) and (*b*).

The curves drawn in Figs. 6, 8, and 9, along with the model parameters listed in Table IV, were computed using the Marquardt algorithm (28), a generalized program for nonlinear least squares curve fitting. The program is available under IBM SHARE Distribution No. 3094, and was run on the Yale Computer Center IBM 7094/7040 system.

Buffers The majority of experiments were carried out at pH 8 in a standard buffer solution containing 30 mM *N*-2-hydroxyethylpiperazine-*N'*-2-ethanesulfonic acid (HEPES; pK_a = 7.48, reference 16; Calbiochem, Los Angeles, Calif.), brought to an initial pH near 8.2 with 25 mM NaOH, and 1% glucose. Acid released by *Neurospora* at this pH is sufficient to reduce the external pH to 7.95–8.05 during the 20 min of preincubation, with normal cell densities of 2 mg dry/ml. After addition of potassium, the pH continues to fall at essentially the same rate; but more than 85% of the total net potassium uptake occurs with the extracellular pH between 8.00 and 7.85. As the experiments progressed, it became clear that small pH changes, within the range 8.5 to 7.5, had very little effect on the net fluxes of sodium and potassium ions (see Fig. 7), and more elaborate methods of pH control were found unnecessary. At lower pH's acid release and therefore pH drift were less rapid.

Other buffers used for measurement of fluxes over the pH range 3.5 to 9.5 were: 15–20 mM 3,3-dimethylglutaric acid (DMG; pK_a's = 3.66 and 6.20, reference 10; Eastman Organic Chemicals, Rochester, N.Y.; used from pH 3.5 to 6.7); 20 mM

N-tris(hydroxymethyl)methyl-2-aminoethanesulfonic acid (TES; pK_a = 7.4, reference 16; Calbiochem; used at pH 7.0); 30 mM glycylglycine (pK_a's = 3.06 and 8.13, reference 5; Nutritional Biochemicals, Cleveland, Ohio; used from pH 8.1 to 9.1); and 68 mM glycine (pK_a's = 2.34 and 9.60, reference 5; Nutritional Biochemicals; used at pH 9.5). In all cases the final Na concentration was adjusted to 25.0 mM, and 1% glucose was added.

Control experiments showed that both HEPES and DMG, the two main buffers, are metabolically inert. Neither will support growth of *Neurospora* as a carbon source, and neither inhibits growth when added to normal medium at 30 mM. TES, glycine, and glycylglycine were not tested in this regard.

Stability of Intracellular K and Na As a further check on the stability of the cells in these buffers and over the pH range in question, potassium loss by normal cells (in buffers containing 25 mM K) and sodium loss by low K cells (in buffers containing 25 mM Na) were measured. At pH 4 and above, the losses of sodium and potassium were equal, independent of pH, and very slow, averaging only 0.52 ± 0.09 mmole/kg cell water·min. At pH 3.5, net loss jumped to 30 mmoles K/kg cell water·min, and at pH 3.0, about 40 mmoles K or Na/kg cell water·min, which was taken as evidence of cell damage. Suspensions at pH 3.5 or below also became milky and difficult to filter, though cell viability following such treatment was not tested. The result is generally consistent with the fact that *Neurospora* does not acidify its own medium below about pH 4.

Oxygen and H^+ Measurements Oxygen consumption and H^+ release by *Neurospora* were measured simultaneously in light suspensions of cells (0.5 mg dry/ml) held in a closed vessel (35 ml) similar to that described by Pressman (33). The suspension was maintained at 25.0°C ± 0.1°C by water circulating in an outer jacket of the vessel, and was stirred with a magnetic flea. Cell clumping under these conditions was prevented by using younger (shorter) cells, grown 9–12 hr in the shaking liquid cultures. A Clarke-type oxygen electrode (Radiometer No. 5093, The London Company, Westlake, Ohio) was employed; it was calibrated against a dense cell suspension, for zero oxygen, and against air-saturated (CO_2-free) buffer, for 0.21 atm. oxygen. The solubility coefficient, α, of oxygen in the buffer was assumed to be the same as in distilled water, 28.31 μl O_2/ml water (47). This has been found to be approximately 8% too large because of the effect of other solutes on oxygen solubility (4), but the discrepancy does not affect the nature of the conclusions. A pH electrode–reference electrode combination unit (A. H. Thomas, Philadelphia, Pa., No. 4858-L15) was used to monitor pH, with a precision of 0.002 pH unit. Leakage of KCl from the reference electrode was less than 100 μmoles/hr and did not interfere with the potassium flux measurements. Simultaneous measurements of H^+ release and net K or Na movement were made by mounting the above pH electrode in a sidearm of the shaking flasks, as described previously (40).

RESULTS

Net K and Na Transport at pH 8 When 30 mM KCl is added to a suspension of low K cells that have been allowed to equilibrate in pH 8 buffer, there

is a rapid net uptake of potassium ions—restoring the intracellular concentration nearly to the normal level in 40 min—and a somewhat slower release of sodium ions (Fig. 1, Table I). In earlier experiments at pH 5.8, K and Na movements were found to be simple exponential functions of time (40), but this is not the case at pH 8. A semilogarithmic plot of the data reveals that, under these new conditions, both fluxes can be resolved into two exponential functions with clearly distinct time constants (Fig. 2).

It is evident from the inset in Fig. 2 that the initial, fast component of potas-

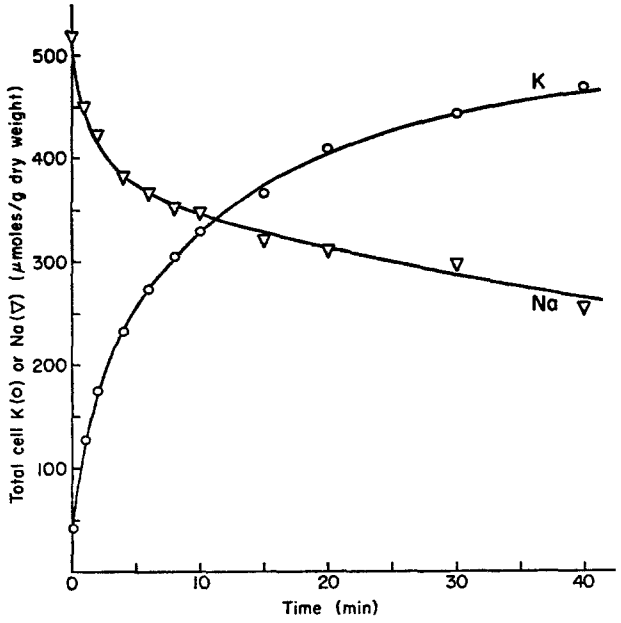

FIGURE 1. Net cation movements in low K cells at pH 8. Cells were grown in 0.2 mM K for 16 hr, and preincubated in K-free HEPES buffer for 20 min at 25°C. The points are averages for duplicate cell samples from a single experiment. The curves are redrawn from the least squares lines in Fig. 2. For potassium, $K_t = 485 - 310\ e^{-t/14.6} - 125\ e^{-t/1.98}$; for sodium, $Na_t = 376\ e^{-t/114} + 125\ e^{-t/1.98}$. The value 485 is the end point for potassium uptake estimated directly from the above data plot.

sium uptake is matched quantitatively by the fast component of sodium loss. The results for 10 experiments show the time constants to be 1.2 ± 0.1 min (for K^+) and 1.4 ± 0.3 min (for Na^+) and the magnitudes to be 118 ± 5 μmoles/g dry (for K^+) and 132 ± 10 μmoles/g dry (for Na^+).

The slow components are not equal, however, with K influx greatly exceeding Na efflux both in amount (259 ± 20 compared with 100 ± 12 μmoles/g dry) and in initial rate (26.2 ± 1.8 compared with 3.5 ± 0.8 μmoles/g dry·min). The question of how electroneutrality is maintained during potassium uptake, whether by release of another cation or uptake of an

TABLE I
TOTAL CELL CATION LEVELS, BEFORE AND AFTER INCUBATION AT pH 8

	Average amounts		No. of experiments
	K	Na	
	μmoles/g dry weight		
Normal cells freshly harvested (16 hr)	458±8	35±3	44
Low K cells, freshly harvested (16 hr)	142±3	252±10	10
Low K cells, preincubated 20 min in K-free HEPES, pH 8	33±5	508±30	8
Low K cells, preincubated, then incubated 40 min in 30 mM K, pH 8	410±23	278±25	8

The K and Na values for normal cells, freshly harvested, are the same as those reported previously (40) in different units: 180 ± 3 mmoles K/kg cell water, and 14 ± 1 mmoles Na/kg cell water.

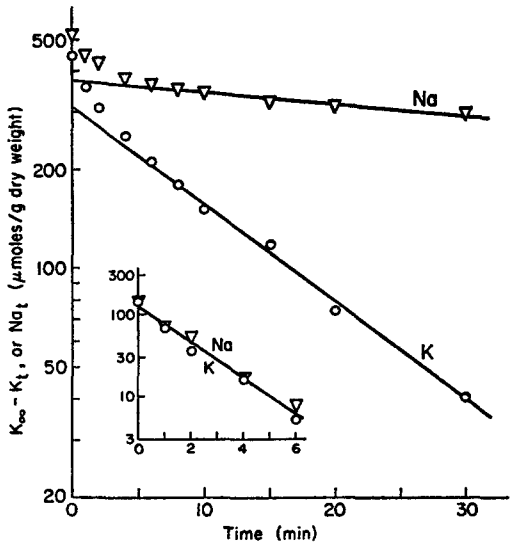

FIGURE 2. Semilog plots of total cell potassium (○) and sodium (▽); the same data as in Fig. 1. In the upper two curves, $(K_\infty - K_t)$ and (Na_t) are plotted, along with the least squares lines computed for data from 6 to 30 min, indicating the slow components of K uptake and Na release. Intercepts and time constants for the two lines are as follows. K, 310 ± 12 μmoles/g dry wt., and 14.6 ± 0.5 min. Na, 376 ± 7 μmoles/g dry wt., and 114 ± 14 min. The inset graph represents the fast components, obtained by subtracting the above least squares lines from the data for times 0–6 min. The results for sodium and potassium are superimposable, and the common least squares line for the fast components has an intercept of 125 ± 10 μmoles/g dry wt., and a time constant of 1.98 ± 0.10 min.

anion, will be dealt with in a later section. In the meantime, we shall be concerned with distinguishing between the fast and slow components, and characterizing them with respect to energy requirements and dependence upon the extracellular potassium concentration.

Energy Dependence The cell wall of *Neurospora* is composed mostly of neutral polysaccharides and does not contain the uronic acids common in higher plants. Work in several laboratories (25–27) has pointed to the presence of some negatively charged amino acids and phosphate residues within the wall, however, and it seemed possible that the fast component of flux might represent a stoichiometric exchange of newly added potassium ions for sodium which had been bound to the cell wall during the preincubation period. Considered simply, this case would require the fast component to be independent of metabolic energy, and therefore to be relatively insensitive to temperature changes and to metabolic inhibitors.

As shown in Fig. 3 *a*, lowering the temperature to 0°C had a relatively small effect on the fast component of K/Na exchange, compared with its pronounced effect on the slow component of potassium uptake. The initial rates and time constants for three experiments, computed from semilogarithmic plots of the data, are averaged in Table II. The initial rate of potassium up-

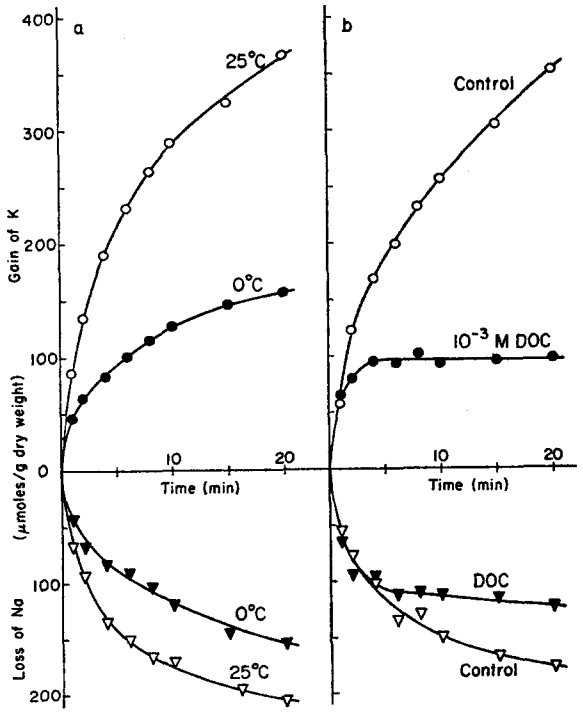

FIGURE 3. Effects of low temperature (*a*) and deoxycorticosterone (*b*) on net cation movements at pH 8. Low-K cells were preincubated 10 min in the usual HEPES buffer at 25°C, and then (at −10 min) either the temperature was reduced to 0°C (*a*) or 10^{-3} M DOC in 1% alcohol was added (*b*). 1% alcohol alone was added to the controls in *b*. 30 mM KCl was added to each flask at 0 time. All points are averages for duplicate cell samples from a single experiment. Mean computed time constants for three sets of experiments are given in Table II.

TABLE II

EFFECT OF 0°C AND METABOLIC INHIBITORS ON POTASSIUM UPTAKE AND SODIUM RELEASE

	Control		0°C		CN^-, $1-3 \times 10^{-3}$ M		DOC, 10^{-3} M	
	K	Na	K	Na	K	Na	K	Na
Fast component								
Initial rate, *μmoles/g dry·min*	98.6 ± 13.2	−94.5 ± 23.9	39.4 ± 7.9	−41.2 ± 5.6	18.8 ± 2.5	−20.1 ± 7.1	86.3 ± 7.6	−87.5 ± 7.4
Time constant, *min*	1.2 ± 0.1	1.4 ± 0.3	2.4 ± 0.3	2.2 ± 0.3	5.6 ± 0.6	4.0 ± 1.1	1.3 ± 0.2	1.4 ± 0.4
Slow component								
Initial rate, *μmoles/g dry·min*	26.2 ± 1.8	−3.5 ± 0.4	2.8 ± 0.2	−2.8 ± 0.2	1.5 ± 1.3	−3.1 ± 0.3	0	−1.3 ± 1.0
Initial rate, *mmoles/kg cell water·min*	10.3 ± 0.7	−1.4 ± 0.3	1.1 ± 0.1	−1.1 ± 0.1	0.6 ± 0.5	−1.2 ± 0.1	0	−0.5 ± 0.4
Time constant, *min*	10.9 ± 0.7	106 ± 13	90 ± 9	112 ± 5	>200	103 ± 3	>300	127 ± 10

take in the slow process was reduced from 26.2 μmoles/g dry·min at 25°C to 2.8 μmoles/g dry·min at 0°C, for an over-all Q_{10} of 2.44. For the fast component, the reduction was significantly smaller, from 96 μmoles/g dry·min (average for K and Na) to 40 μmoles/g dry·min, to give an over-all Q_{10} of 1.42. This latter figure is well within the range of temperature coefficients for typical ion exchange resins (19). [The still smaller apparent reduction in the slow component of Na release at 0°C is increased somewhat by allowing for loss of sodium which could occur in the absence of external potassium (0.5 mmole/kg cell water·min; see Methods); the relatively small size of sodium flux at pH 8, however, makes it difficult to determine with accuracy.]

The standard respiratory inhibitors turned out not to be very useful in distinguishing between the fast and slow components of cation movement in *Neurospora*. Azide and dinitrophenol, which have pK_a's of 4.72 and 3.96 (48) respectively, are taken up by cells primarily in the unionized form (22). At pH 8 they would be expected to enter *Neurospora* only very slowly and—at reasonable extracellular concentrations—to have very little effect on respiration or ion transport. This latter expectation was borne out by experiments. Cyanide, however, should be more potent than the other inhibitors at pH 8, since its pK_a is 9.31 (48). Indeed, concentrations of sodium cyanide (1 mM or above) which blocked 98% of respiration in *Neurospora* were found to inhibit essentially all of the slow component of potassium uptake. The rapid exchange was still observed after exposure to cyanide, although its time constant was increased from 1.2 to 5.6 min. The reasons for this effect are not clear, but may reflect some secondary action of cyanide on the wall at high concentration.

The inhibitor which has been most useful in distinguishing between fast and slow fluxes is deoxycorticosterone which, at 10^{-3} M, blocks the slow potassium uptake completely and leaves the fast K/Na exchange quantitatively unaltered (Fig. 3 *b*, Table II). DOC has long been considered a generalized inhibitor of membrane transport in *Neurospora*. Lester, Stone, and Hechter (24) presented evidence to suggest that it interfered with uptake of sugars, amino acids, and rubidium ions by germinated conidia. It was also said to reduce oxygen consumption, but only that fraction resulting from the utilization of exogenous sugars. Our control experiments have not borne out this latter finding: DOC at 10^{-3} M was found to reduce oxygen consumption by 40–45% at both pH 5.8 and 8, regardless of whether added glucose was present in the medium; added glucose was found to increase oxygen consumption by 15–20% at both pH's, regardless of whether DOC was present. However, there is no doubt that the effect of DOC on respiration is relatively much smaller than its effect on the slow component of K uptake. Fig. 4 shows that concentrations between 3×10^{-5} M and 10^{-3} M progressively blocked the slow component of K uptake at pH 8, while causing only a 30% inhibition of oxygen consumption. The same concentrations also have been found to inhibit

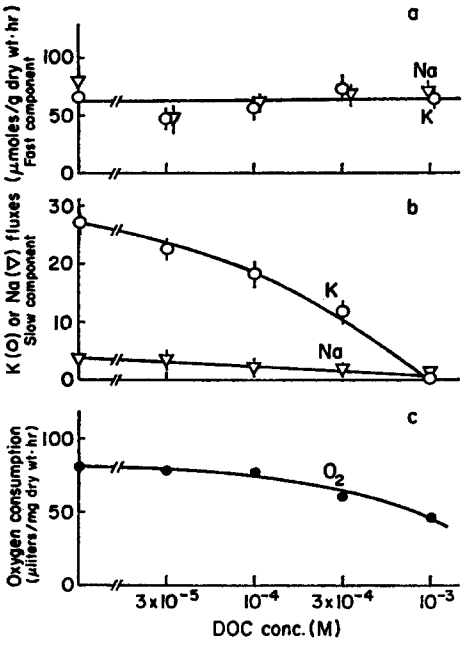

FIGURE 4. Effect of varying DOC concentrations (0–10^{-3} M) on the fast (*a*) and slow (*b*) components of net cation fluxes, and on oxygen consumption (*c*), at pH 8. For flux measurements the cells were handled as in Fig. 3, with DOC being added at −10 min. For zero DOC, 1% alcohol alone was added to the suspensions. Separate aliquots of cell suspension were used for the oxygen measurements, which were made with a Clarke-type oxygen electrode (see p. 761). Addition of 30 mM KCl, per se, had no measurable effect on the rate of oxygen consumption. Vertical bars, ± 1 SE.

net K and Na movements and the steady-state K/K exchange at pH 5.8[1], again with significant but smaller effects on respiration. By contrast, the rapid K/Na exchange is independent of DOC concentrations as high as 10^{-3} M (Fig. 4).

The results at 0°C and those in the presence of DOC or cyanide strongly indicate that the slow potassium uptake at pH 8, like the steady-state K/K exchange (42) and the net movements of sodium and potassium (40) at pH 5.8, requires metabolic energy. For the fast component of K/Na exchange at pH 8, the data are less clear. The effect of DOC suggests that the fast component is not dependent on metabolism, and the temperature results are consistent with this interpretation, while the cyanide effect is contradictory. Despite this inconsistency, the simplest and generally most satisfactory way to interpret the inhibitor results is to suppose that the rapid K/Na exchange at pH 8 is nonmetabolic, probably taking place extracellularly on negatively charged groups in the cell wall, while the slower K uptake represents energy-dependent entry into the cytoplasm. Evidently, a precise interpretation is contingent upon whether the two cellular compartments—which are reflected by the fast and slow components of K movement—are viewed as functionally parallel or functionally in series.

Curve Analysis: Series- and Parallel-Compartment Models Identification of the two separate exponential components of the potassium curve (or sodium curve) in Figs. 1 and 2 with two separate cellular compartments requires that

the compartments be arranged in parallel and have independent access to the external medium. If this underlying assumption is not valid, so that potassium must pass through the postulated fixed charge regions of the cell wall before it reaches the cell membrane (series arrangement), then—as has been pointed out by several authors, e.g., Solomon (44)—elements from both real compartments will appear in each of the graphically separated flux curves. This could, superficially at least, account for the increased time constant of the fast component (5.6 sec, instead of 1.2 sec; see Table II) of potassium uptake seen with cyanide. Quantitative considerations make this explanation rather unlikely, however.

Calculations based on the series arrangement (detailed in the Appendix; see Table V) show that the characteristic rate constant (reciprocal of the time constant) for entry into the wall would be overestimated by 17% and the amount of potassium entering would be underestimated by 29% in the curves of Fig. 2. The effective removal of the intracellular compartment by metabolic inhibitors should produce compensatory changes in the fast component. Table II shows that cyanide does reduce the rate constant of the fast component, but by 80% rather than 17% ($1/5.6 = 0.179$ min^{-1}), while it has no significant effect on the magnitude of the fast component. The action of cyanide thus remains paradoxical. The action of DOC is simpler, showing no influence on either the rate constant or the magnitude of the fast component.

The latter result might be taken as evidence that the two compartments lie functionally in parallel, so that small ions can get to the cell membrane of *Neurospora* without passing through fixed charge regions of the wall. This possibility is further supported by the finding that polymers of ethylene glycol and dextran with molecular weights up to 4700 pass readily through the *Neurospora* wall (46), as do secreted enzymes with much larger molecular weights (14, 29, 46). It is likely, then, that the cell wall is laced with water-filled pores, and pores as large as 40 A in diameter have been tentatively identified in electron micrographs of the *Neurospora* wall (27). For these reasons, we have carried out the further analysis of K and Na fluxes at high pH assuming a parallel, rather than a series, arrangement of (fixed charge regions of) the cell wall and cytoplasm. Consequences of the opposite assumption are analyzed in the Appendix; it has no important qualitative effect on the results.

Properties of the Nonmetabolic K/Na Exchange The dependence of the fast, DOC-insensitive K/Na exchange on the extracellular potassium concentration is illustrated in Fig. 5. At all concentrations, the amount of potassium taken up equals the amount of sodium released, and both increase along a standard ion exchange isotherm as external potassium is raised from 0 to 60 mM, with external sodium held constant at 25 mM. From a Scatchard plot of the same data (inset, Fig. 5), the potassium concentration (α) required for half-displacement of sodium can be calculated as 32.0 ± 3.4 mM, so that the

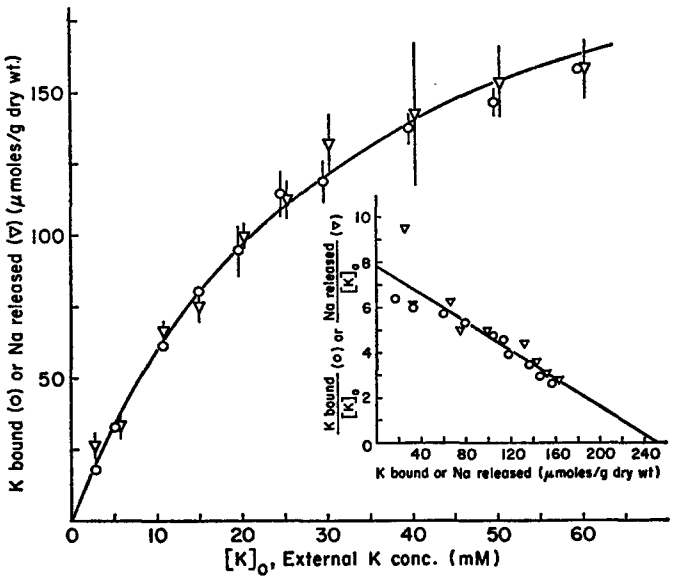

FIGURE 5. The fast component of K/Na exchange at pH 8, plotted as a function of the extracellular K concentration. Low K cells were suspended in HEPES buffer to which 10^{-3} M DOC in 1% alcohol had been added, to inhibit the slow component of K/Na exchange. After the usual 20 min preincubation, KCl (2–60 mM) was added, and cell samples were collected at 0, 1, 2, 4, 6, 8, and 10 min. Each point represents averages for data from three separate experiments. Vertical bars, ± 1 SE. The curve is drawn according to the ion exchange isotherm,

$$B = \frac{B_{max}\,[K]_o}{\alpha + [K]_o}$$

where B is the amount of K bound or Na released, B_{max} is the maximal amount of cation that can be bound, and the constant α corresponds to the value of $[K]_o$ at which the binding sites are half-filled by potassium. The *inset* shows a Scatchard plot ($B/[K]_o$ vs. B) of the results, with the straight line fitted by the method of least squares. From the intercepts of this line, B_{max} = 251 ± 30 μmoles/g dry wt., and the calculated α equals 32.0 ± 3.4 mM. The curve in the main part of this figure is redrawn from the inset, using the estimated values of B_{max} and α.

selectivity of the postulated binding sites for sodium over potassium is barely significant. The maximum amount of cation which can be bound (B_{max}) at pH 8 is 251 ± 30 μmoles/g dry cells. If this corresponds to negatively charged sites distributed evenly throughout the cell wall, and if the cell wall is assumed to occupy 20% of the total cell volume (11, 39; the wall forms a layer 0.1 μ thick around a cylinder 1 μ in radius), then the charge density would be 1250 μmoles/g dry wall, or 500 mmoles/liter wall water, assuming that the wall water is 2.54 times the wall dry weight (see Methods for the conversion factor).

Fig. 6 shows the magnitude of the K/Na exchange as a function of pH. Below pH 5.8 (the pH of the usual growth medium, and therefore that used in all previous experiments, references 40 and 42), exchange is negligible. As the incubation medium is made more alkaline, exchange increases until it reaches a maximum at pH 8.5–9. Half-maximal exchange is seen at approximately pH 7.1. These results suggest the titration of weakly acidic groups, unionized at low pH and therefore not affecting the K/Na flux

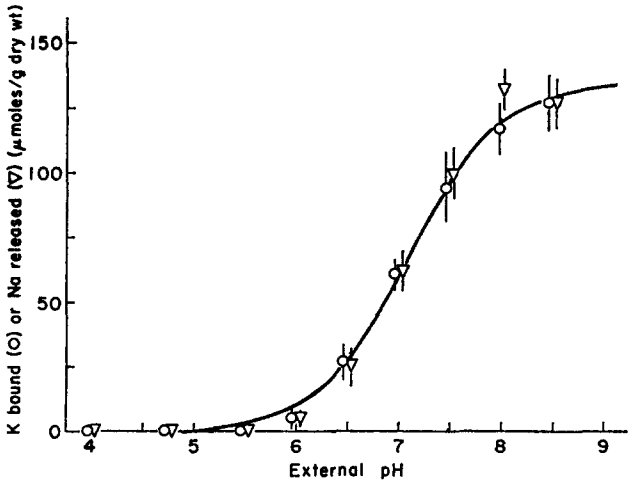

FIGURE 6. pH-dependence of the fast component of K/Na exchange. Standard low K cells were preincubated 20 min in Na buffer at various pH's before addition of 30 mM KCl. Each point is the mean of three to five experiments. Vertical bars, ± 1 SE. The curve is drawn according to the equation $K_{bound} = Na_{released} = 136\ X^-$, where 136 μmoles/g dry wt. is the asymptote at high pH, and X^- is the fraction of sites which are actually dissociated at a given pH. X^- is defined by the Henderson-Hasselbach equation: $pH = pK + \log\frac{X^-}{1 - X^-}$, with pK = 7.1. Curve fitted by means of the Marquardt algorithm (see Methods).

measurements, but progressively ionized—and capable of binding Na or K—at higher pH.

The data are reasonably well-fitted by a simple titration curve, the Henderson-Hasselbach equation, with an apparent $pK_a = 7.1$. One would expect a typical weak-acid resin to establish a Donnan regime, however, with the pH inside the resin matrix depressed below the pH of the external medium (19). This should have two consequences: (*a*) The inflection point of the titration curve should not give the real pK_a for dissociation of the weak-acid sites. Instead, for a resin with a fixed charge density of 500 mmoles/liter water and an apparent pK_a (referred to the pH of the medium) of 7.1, the real pK_a of the sites would be about 6.4, as calculated from the Donnan

theory (19). (*b*) In addition, the titration curve would be expected to spread out along the pH axis, since the Donnan potential would drive in hydrogen ions (as well as K and Na), thereby tending to reduce dissociation of the fixed charges. Preliminary calculations indicate that this effect would diminish the steepest slope by 30%, for a site density of 500 mmoles/liter. Failure to observe such spread might indicate cooperative interactions between adjacent dissociable sites (37), but a quantitative development of this notion would be premature in the absence of precise measurements on isolated cell wall material.

Potassium and Sodium Transport As a Function of pH We now turn to the slow component of potassium and sodium fluxes. Fig. 7 shows the pH-dependence of net K influx and net Na efflux once the nonmetabolic exchange has been subtracted at all pH's where it is significant. Between pH 4 and 6, potassium uptake is rapid and essentially constant, having a velocity of approximately 19 mmoles/kg cell water·min, with external potassium at 30 mM. It is balanced largely by sodium efflux at approximately 14 mmoles/kg cell water·min, and the difference is made up quantitatively by the release

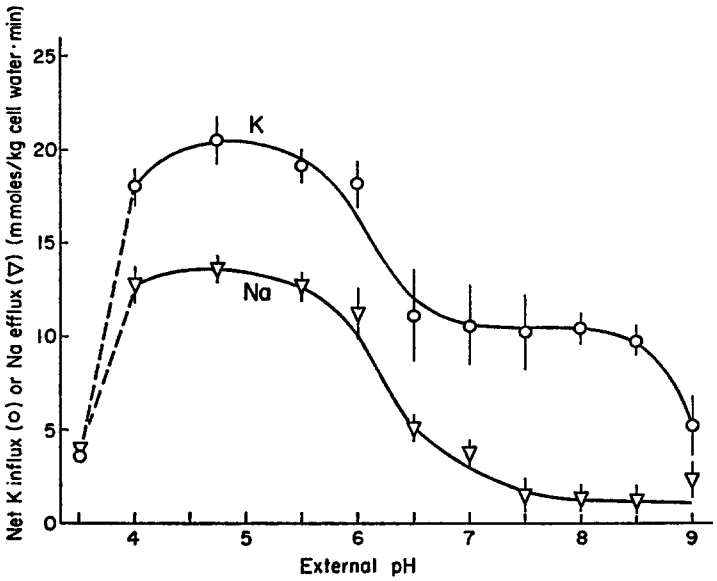

FIGURE 7. Net potassium influx (○) and sodium efflux (▽), as a function of extracellular pH; fast component subtracted. These are the initial rates of the slow components of K uptake and Na release, calculated from semilog plots as in Fig. 2. Standard low K cells, preincubated 20 min in Na buffer before addition of 30 mM KCl. Maximal fluxes at saturating K concentrations would be somewhat higher (see text). Each point represents the mean value of three to five experiments. Vertical bars, ± 1 SE. As has already been noted (see Methods), the values at pH 3.5 do not represent physiological fluxes, because of generalized breakdown of the cells at this pH.

of hydrogen ions (40). All three fluxes (K influx, Na efflux, H efflux) can be accounted for in terms of a single pump displaying standard Michaelis-Menten kinetics. The $K_{1/2}$ for extracellular potassium is 11.8 ± 1.1 mM at pH 5.8 (40) and 11.3 ± 0.9 mM at pH 4.0;[1] and the corresponding maximal velocities are 23.6 ± 0.7 and 22.7 ± 0.5 mmoles/kg cell water·min.

Above pH 7, there is a marked change in the net fluxes. Potassium uptake is reduced by roughly 50%; but more important, sodium release is nearly abolished, being reduced to a level (1.4 ± 0.3 mmoles/kg cell water·min) only slightly greater than that expected from passive leak alone. The discrepancy between net potassium influx and net sodium efflux at pH 8, 8.9 ± 0.5 mmoles/kg cell water·min, has not yet been definitely accounted for. The observed K-induced stimulation of H^+ release at pH 8 was 2–4 mmoles/kg cell water·min, barely significant against a base line release of 20–30 mmoles/kg cell water·min. It is possible that initiation of net potassium uptake leads to a switching off of part of the organic anion secretion which accompanies base line H^+ release, as has been found in yeast (6), so that the hydrogen ions then serve to balance a large fraction of potassium uptake. Methods are now being developed to measure the organic anions released, and it should be possible to test this aspect of the hypothesis within the near future.

Indirect evidence that the efflux of hydrogen or some other cation must balance potassium influx at high pH comes from the demonstration that anion movements are negligible (Table III). Although ^{36}Cl, $^{32}PO_4$, and $^{35}SO_4$ are taken up by *Neurospora* at pH 8, the influxes are less than 2.1 mmoles/kg cell water·min at the concentrations used in these experiments, compared with the K-Na difference of 8.9 mmoles/kg cell water·min. Furthermore, the anion fluxes are the same whether or not the cells are taking up potassium (fourth column, Table III). Participation of the buffer anion (HEPES) has not been ruled out directly, but flux experiments conducted in the absence of

TABLE III

ANION INFLUXES INTO LOW K CELLS, pH 8

Tracer anion	K or Na added as	Initial fluxes	
		K salt	Na salt
		mmoles/kg cell water·min	
^{36}Cl	Cl (30 mM)	2.1	1.8
$^{32}PO_4$	PO_4 (15.5 mM)	0.56	0.48
$^{35}SO_4$	SO_4 (15 mM)	0.093	0.093

In all cases the cells were preincubated in the standard buffer, 25°C. Tracer was added along with 30 mM K or Na, and uptake of label was followed for 40 min.

buffer (in a pH stat) show the same large discrepancy between potassium and sodium movements.

Dependence of Transport at pH 8 on the Extracellular K Concentration In addition to the question of the identity of the exiting cation, there is a second conspicuous difference between potassium transport at high pH and that at low pH. Fig. 8 shows that, with the DOC-insensitive, fast component of K/Na exchange subtracted out, the initial rate of net potassium uptake at pH 8 follows a sigmoid curve as a function of the extracellular potassium concentration. And a double reciprocal plot of the same data gives a curve

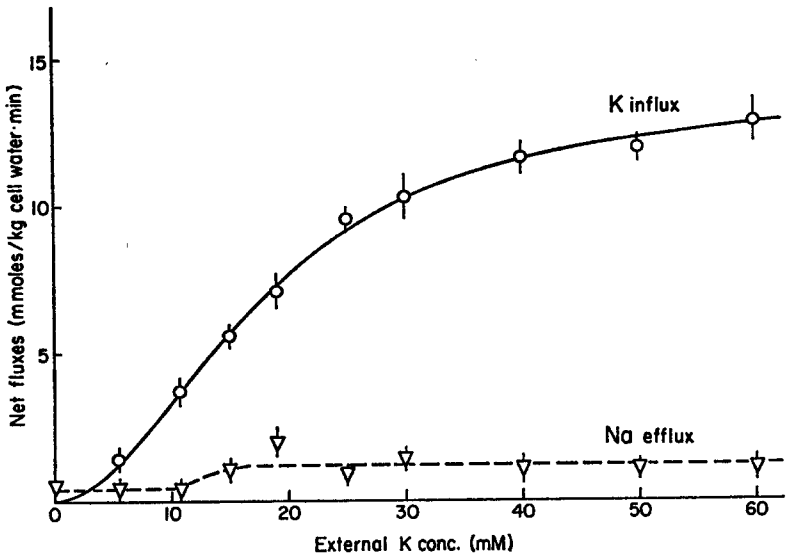

FIGURE 8. Dependence of net cation fluxes at pH 8 on the extracellular potassium concentration; fast component subtracted. Standard low K cells preincubated 20 min in HEPES buffer, 25°C. KCl added to final concentrations of 5–60 mM. Fluxes were calculated from semilog plots of the data, either by separating the fast and slow components graphically (Fig. 2) or by subtracting the DOC-insensitive K and Na fluxes obtained from a parallel experiment. Both methods gave the same results. The points represent average results from at least three experiments. Vertical bars, ± 1 SE. The curve for potassium is drawn according to equation 2, with P_2 = 13.9 (mmoles/kg cell water·min) and P_3 = 317 (mM²; see Table IV).

which is concave upward, rather than the usual straight line (Fig. 9 *a*). Such findings suggest a multisite transport system, in which more than one site on the carrier can react with extracellular potassium during the transport process. In fact, as shown below the data at pH 8 can be fitted very well by assuming that the carrier has two sites for potassium.

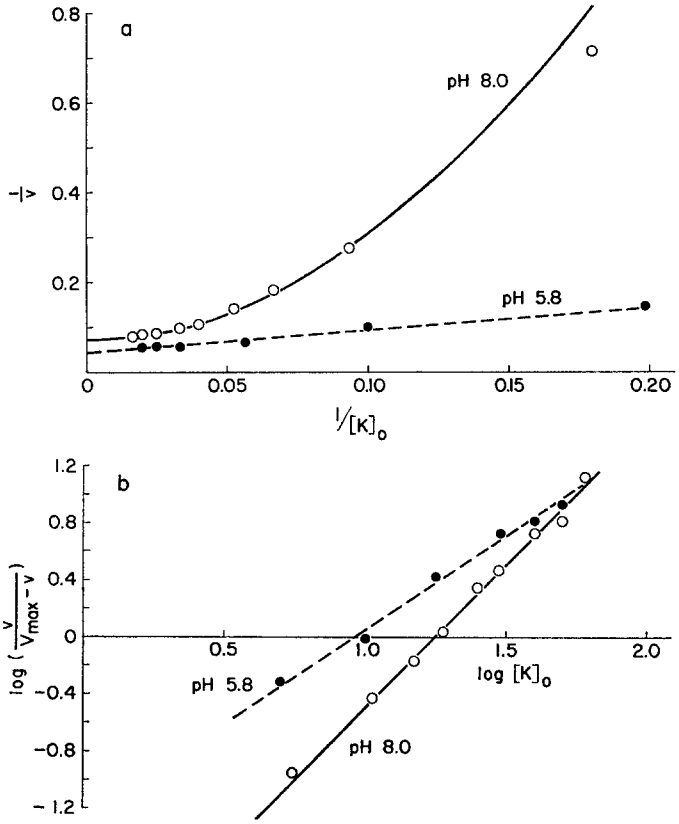

FIGURE 9. Dependence of net potassium influx on the extracellular potassium concentration; fast component subtracted. *a*, Double reciprocal plots, with curves drawn according to equation 3 for pH 8 and the Lineweaver-Burk equation for pH 5.8, using the parameters from Table IV. *b*, Hill plots, with curves drawn according to equation 5, again using the parameters listed in Table IV.

Two-Site Rate Equations The most general reaction sequence which need be considered is the following:

A.

$$E + S \underset{k_{-1}}{\overset{k_1}{\rightleftharpoons}} ES \xrightarrow{k_5} E + P \qquad K_x = \frac{k_{-x}}{k_x}$$

$$E + S \underset{k_{-2}}{\overset{k_2}{\rightleftharpoons}} SE \xrightarrow{k_6} E + P$$

$$ES + S \underset{k_{-3}}{\overset{k_3}{\rightleftharpoons}} SES \xrightarrow{k_7} ES + P$$

$$SE + S \underset{k_{-4}}{\overset{k_4}{\rightleftharpoons}} SES \xrightarrow{k_8} SE + P$$

[The binding reactions involve an element (E) of the carrier system, presumably located at the outer surface of the membrane, and the substrate (S, in this case extra-

cellular potassium). The ensuing reactions: translocation across the membrane, breakdown of the complex to form product (P, in this case intracellular potassium), and return of the carrier to the initial condition, are all lumped together and designated by rate constants $k_5 - k_8$. For mathematical convenience, at least one reaction of each set is assumed to be irreversible. The symbols, E, S, and P, and their combinations will be assumed to represent concentrations. Constants designated K_x represent equilibrium constants; k_x, individual rate constants.]

In the general reaction sequence outlined above, two sites on the enzyme are postulated to react, in any order, with the substrate, and then to break down, also in any order. If the breakdown reactions are assumed to be relatively rapid ($k_5 - k_8$ large) and the system is analyzed under steady-state conditions (13), the over-all reaction velocity is third-order in S and contains six coefficients which need to be determined. On the other hand, when $k_5 - k_8$ are assumed to be small, so that the binding reactions may be considered at equilibrium, then the reaction velocity simplifies to an equation of the form:

$$v = \frac{P_1 \cdot S + P_2 \cdot S^2}{P_3 + P_4 \cdot S + S^2}; \qquad (1)$$

where $P_1 = (k_5K_3 + k_6K_4)\, E_T$; $P_2 = (k_7 + k_8)\, E_T = V_{max}$; $P_3 = K_1K_3$; $P_4 = K_3 + K_4$; and E_T designates the sum of all forms of the enzyme present, which is assumed to be constant.

If the ternary intermediate, SES, is substantially more reactive than either of the binary intermediates, then the reaction velocity will be a sigmoid function of the substrate concentration. This mechanism implies that the binding of a second substrate molecule to the carrier induces a conformational change that increases its ability to move across the cell membrane and release product on the other side.

B. Alternatively, one might imagine that the uncombined carrier itself can exist in two conformations which are in equilibrium with each other, and that binding of one substrate molecule to the carrier shifts the equilibrium toward the more active conformation, resulting in an increase in the effective concentration of enzyme. If all the reactive sites on any one carrier molecule are assumed to be identical and independent, the system is described by the allosteric model of Monod, Wyman, and Changeux (30).

$$E_r \overset{L}{\rightleftharpoons} E_t \qquad L = \frac{E_t}{E_r}$$

$$E_r + S \overset{K_r}{\rightleftharpoons} E_rS \qquad E_t + S \overset{K_t}{\rightleftharpoons} E_tS$$

$$E_rS + S \overset{K_r}{\rightleftharpoons} SE_rS \qquad E_tS + S \overset{K_t}{\rightleftharpoons} SE_tS$$

$$E_rS \xrightarrow{k_p} E_r + P$$

$$SE_rS \xrightarrow{k_p} E_rS + P$$

For simplicity, we have assumed that one form of the enzyme (E_t) is catalytically inactive (though it may still bind substrate) and that the binding reactions are in equilibrium. From equation (2) of Monod et al. (30), the fraction of sites which are occupied in the active form is

$$F_r = \frac{\frac{S}{K_r}\left(1 + \frac{S}{K_r}\right)}{L\left(1 + \frac{S}{K_t}\right)^2 + \left(1 + \frac{S}{K_r}\right)^2}$$

And the over-all reaction velocity is given by $v = k_P \cdot 2E_T \cdot F_r$, where E_T again is the sum of all forms of the enzyme. This equation readily rearranges into the form of equation 1, in which the coefficients $P_1 - P_4$ are rather complicated functions of K_t, K_r, and L.

Evaluation of the Data Computer estimates for the four parameters $P_1 - P_4$ are shown in Table IV (line 1); the fit is quite satisfactory, though as seen from the standard errors, both P_1 and P_4 could be zero. [The negative value for P_4 has no physical meaning.] In terms of model (A) discussed above, $P_1 = 0$ would mean that the binary intermediates could not break down to form product ($k_5 = k_6 = 0$). In (B), P_1 cannot equal zero, but a very small value would imply that substrate is tightly bound to the active conformation of the enzyme (K_r very small).

If P_1 and P_4 are assumed to be zero, equation 1 reduces to

$$v = \frac{P_2 \cdot S^2}{P_3 + S^2}, \tag{2}$$

which could arise from the following reaction sequence:

$$E + 2S \underset{k_{-1}}{\overset{k_1}{\rightleftharpoons}} SES \xrightarrow{k_2} E + 2P.$$

TABLE IV

PARAMETER ESTIMATES FOR RATE EQUATIONS

pH	Equation	Parameters					Σd^2
		P_1	P_2	P_3	P_4	P_5	
8.0	1	44.2 ± 55.0	12.6 ± 1.4	457 ± 162	−4.43 ± 4.96	—	0.291
8.0	2	—	13.9 ± 0.2	317 ± 15	—	—	0.349
8.0	4	—	13.8 ± 0.4	325 ± 97	—	2.01 ± 0.12	0.348
5.8	Michaelis	23.3 ± 1.0	—	11.9 ± 1.5	—	—	1.79
5.8	4	20.5 ± 1.2	—	19.2 ± 6.2	—	1.32 ± 0.19	0.98

The data used to evaluate all parameters at pH 8 were those plotted in Fig. 8. For pH 5.8, the data were taken from reference 40 (Fig. 8). All values are least squares estimates (± 1 SE) obtained by computation with the Marquardt algorithm (28). $\sum d^2 = \sum$ (predicted value − observed value)^2 for all points; 10 average data points were used at pH 8, and 7 at pH 5.8. The maximal net influx (V_{max}), in units of mmoles/kg cell water·min, is given by P_2 for pH 8, and by P_1 for pH 5.8. The potassium concentration required for half-maximal flux ($K_{1/2}$), in mmoles/liter, is equal to P_3 at pH 5.8 (Michaelis equation) and to $(P_3)^{1/2}$ at pH 8 (equation 2).

This case is obviously analogous to the Michaelis equation, except that S is replaced by S^2. There is no binary intermediate; instead the ternary complex between the enzyme and two substrate molecules arises from a three-way collision. $P_2 = k_2E_T = V_{max}$, and $P_3 = \frac{k_{-1}+k_2}{k_1}$ or $\frac{k_{-1}}{k_1}$ under steady-state or equilibrium conditions, respectively. Models involving three-way collisions seem rather improbable, however, and equation 2 can more rationally be viewed as an approximate description of the variety of possible two-site models encompassed by (A) and (B) above. Under any of these models P_2 represents the maximal transport velocity, but no definite physical meaning can be attached to P_3, unless equation 2 is taken literally, in which case $P_3 = (K_{1/2})^2$.

Computer estimates of P_2 and P_3 are given in line 2 of Table IV. Because the quality of fit (as judged by $\sum d^2$, last column) is nearly as good as with equation 1, the simpler equation can be used for purposes of further calculation.

Equation 2 is readily converted to the double reciprocal form, so that

$$\frac{1}{v} = \frac{1}{V_{max}}\left(1 + \frac{P_3}{[K]_o}\right) \tag{3}$$

can be used to describe the parabola in Fig. 9 *a*. A double reciprocal plot of the results at pH 5.8 (40) is shown (dashed line) for comparison in Fig. 9 *a*.

Hill plots, in Fig. 9 *b*, indicate the extent to which the data on net potassium influx satisfy one-site and two-site models, respectively, at pH 5.8 and 8. Equation 2 is rewritten:

$$v = \frac{P_2[K]_o^{P_5}}{P_3 + [K]_o^{P_5}} = \frac{V_{max}[K]_o^{P_5}}{P_3 + [K]_o^{P_5}} \tag{4}$$

where P_5 = the number of substrate molecules involved, under model (A); and is a related thermodynamic quantity (49) under model (B). The equation can be linearized for plotting:

$$\log \frac{v}{V_{max} - v} = P_5 \log [K]_o - \log P_3 \tag{5}$$

in which P_5 becomes the slope of the log-log plot. At pH 5.8, the Hill plot of data shows fair agreement with the Michaelis equation: the least squares estimate of the slope is 1.32 ± 0.19 (instead of 1). At pH 8, the least squares estimate of P_5 is 2.01 ± 0.12, essentially identical to 2; and the other parameters also turn out to be very close to those obtained from equation 2.

Again it should be noted that the assumption of a series-compartment arrangement for the cell wall and cytoplasm would not affect the basic sigmoid shape of the velocity curve, although it could lead to a 20–30%

underestimate of the maximal transport velocity and a much larger underestimate of the potassium concentration required to produce half the maximal velocity. The appropriate computations are outlined in the Appendix, and listed in Tables V and VI.

The over-all conclusion from this portion of the results seems clear: that potassium transport at pH 5.8 can be adequately accounted for in terms of a classical one-site carrier obeying Michaelis kinetics (40), but transport at pH 8 requires at least two sites for potassium. It is not possible, from present data, to specify whether the two sites are identical or different, whether they are loaded simultaneously or sequentially, or whether the sigmoid shape arises from mechanism (A) or mechanism (B).

DISCUSSION

Cell Wall At pH 8 the uptake of cations by *Neurospora* resembles, in the sense of showing two distinct components, observations made widely on microbial and plant cells. The giant algae (8, 12) and tissues of higher plants (3) show an initial fast component of cation uptake that is insensitive to metabolic inhibitors and has a time constant on the order of a minute or less. This fast component has been attributed to ion exchange on fixed charge sites in the cell wall, an idea reinforced in several cases by direct studies on isolated cell wall material. Estimated fixed charge densities run as high as 800 mmoles/ liter cell wall (9). In plant cells, dissociation of carboxyl groups of glucuronic and galacturonic acids—chiefly in pectins—produces negatively charged sites with pK_a's of 2–3 (3, 9). Recent studies of H^+ uptake by walls of bacteria (*Staphylococcus aureus*) have indicated pK_a's of 3.2–4.8, presumed to come from phosphate groups of teichoic acids (15). Phosphate and carboxyl groups have also been implicated in cation binding at the surface of yeast cells (34).

The cell wall of *Neurospora* is composed principally of neutral polysaccharides: chitin (poly-*N*-acetylglucosamine), β-glucan, and polygalactosamine (25–27). The two most likely sources of negatively charged sites within the *Neurospora* wall are relatively minor components, carboxyl residues of proteins and inorganic phosphate and polyphosphate groups, and information so far available on these compounds does not account quantitatively for the ion exchange data. "Insoluble" polyphosphate with a mean chain length of 50 has been found in purified *Neurospora* wall material to the extent of 370 μmoles P/g·dry wall (recalculated from Harold (18), assuming 0.04 g dry wall/g wet mycelium). This amounts to 30% of the fixed charges (1250 μmoles/g dry wall) required by the ion exchange data. But Harold considers the apparent localization of polyphosphate in the wall to be an artifact of the fractionation process, with free cytoplasmic polyphosphate becoming absorbed to the wall only when the cells are disrupted.

A second possibility is protein, which has been reported to constitute 12–

15% by weight of the *Neurospora* wall (25, 27). This protein fraction contains an unusually high proportion of acidic amino acid residues, aspartic and glutamic acids: 17.5% by weight of the total wall protein, or 21–26 mg for each gram of cell wall. This would yield a fixed charge density of 300–375 μmoles/g dry wall, or again, 30% of the total fixed charges needed to account for the ion exchange data. There remains, too, a problem of dissociation constants: the pK_{a2}'s of aspartic and glutamic acids are 3.65 and 4.25, respectively (5), compared with the pK for ion exchange of 6.4–7.1. In some cases the intrinsic dissociation constants for carboxyl residues are known to shift when amino acids are incorporated into protein, but shifts as large as two pH units are rare (45).

Clearly, the best way to obtain direct information about the role of the *Neurospora* cell wall in cation uptake would be to measure the ion exchange properties of isolated cell wall material (attempting to identify chemically any binding sites that were found), and additionally, to determine potassium fluxes in protoplasts (spherical cells from which most of the cell wall has been removed enzymatically).

Transport at High pH The key observation reported in this paper is that, once the ion exchange component has been subtracted, potassium uptake at high pH follows a sigmoid curve as a function of the extracellular potassium concentration. As explained in the Results section, this indicates a multisite transport system in which two or more sites on the carrier can react with potassium during the transport process. It now becomes important to examine the relationship between the multisite kinetics at pH 8 and the standard Michaelis kinetics previously observed for potassium uptake at low pH (40). At least two possibilities could account for these findings:

1. The pH 8 results might reflect a second, previously undetected cation transport system in the *Neurospora* membrane. Net potassium uptake and net sodium and hydrogen ion efflux at pH 4–6 (40), together with steady-state potassium exchange at low pH (42), might be carried out by one system displaying conventional Michaelis kinetics; and potassium uptake at pH 8 by a second, multisite system with a high pH optimum. It should be possible to test this hypothesis by examining a series of cation transport mutants (43). If the *Neurospora* membrane contains two transport systems with different pH optima, then some mutants should be defective in K uptake at low pH, and other mutants at high pH. If, on the other hand, all cation fluxes are mediated by a single system, then most (if not all) transport mutants should show abnormal cation fluxes at all pH's. Experiments of this kind are now in progress.

2. In the absence of conclusive data on transport mutants, it is still reasonable to ask whether a single pump model can be constructed that accounts quantitatively for all the kinetic results (pH 4–8) on wild-type

Neurospora. Two sorts of molecular mechanisms can be obtained by extending the two models described in the Results section, so that a reaction with H^+ (at low pH) causes a shift from sigmoid to standard Michaelis kinetics. In the first (model A), the transport system would contain both a carrier site responsible for potassium uptake, and a modifier site that must be filled with a cation (H^+ at low pH, potassium at high pH) in order for transport to occur. Armstrong and Rothstein (2) have proposed a similar model to explain potassium transport in yeast. The basic experimental observations in yeast are that at high pH, the $K_{1/2}$ (external potassium concentration for half-maximal flux) for potassium uptake is low and the V_{max} is high; at low pH, the V_{max} decreases (interpreted as an effect of H ions at the modifier site) and the $K_{1/2}$ increases (interpreted as competition between H and K at the transport site). Sigmoid kinetics are not seen in yeast at high pH, but in the modifier model this would depend on the exact values of the various reaction constants.

Alternatively an allosteric mechanism (corresponding to model B of the Results section) can be imagined, in which the transport system consists of multiple subunits, each with an active site for potassium. If in addition hydrogen ions are assumed to be allosteric activators of the system (30), this model could generate sigmoid uptake curves at high pH (in the effective absence of hydrogen ions), but standard Michaelis curves at low pH, with hydrogen ions present.

We have made a preliminary attempt to fit both model A and model B to four sets of data on net potassium influx in wild-type *Neurospora*: influx over a range of potassium concentrations at pH 4, pH 5.8 (Fig. 8, reference 40), and pH 8 (Fig. 8, above), and influx over a range of pH's at 30 mM K (Fig. 7, above). Both models are able to fit the data qualitatively. In both cases, however, there are small systematic discrepancies from the data: insufficient sigmoid shape at pH 8, too large V_{max}'s at all pH's, and too gentle a slope in the pH curve. All the discrepancies are diminished by including the unlikely assumption of a simultaneous three-way collision between the carrier and two potassium ions, or by going to three-site models. More data at various potassium, sodium, and hydrogen ion concentrations, and in the presence of other univalent cations, will be required to provide an adequate test of any particular hypothesis.

Evidently, a comprehensive model must also be able to account for the efflux aspects of the transport process, particularly the greatly decreased Na efflux at high pH, shown in Fig. 7. No attempt has been made to incorporate this observation into the models discussed above, since we do not yet know the dependence of Na efflux upon *intracellular* potassium, sodium, or hydrogen ion levels.

The basic observation of a multisite cation transport system in *Neurospora*, whatever the exact mechanism, is not without precedent. In addition to the

findings with yeast (1, 2), Keynes and Swan (21), Mullins and Frumento (31), and Keynes (20) have presented evidence for a three-site carrier involved in sodium efflux from frog muscle (where at low intracellular sodium concentrations, efflux is proportional to the third power of the concentration). In human red blood cells, flux measurements have indicated that two potassium ions are transported inward for every three sodium ions transported outward (32). More recently, Sachs and Welt (36) and Sachs (35) have measured the dependence of active potassium influx on the extracellular potassium concentration, as well as the competitive inhibition of potassium uptake by rubidium, cesium, and lithium; and their results can be interpreted very nicely in terms of a two-site model (35). It will be interesting if multisite cation transport systems turn out to be a general feature of microbial as well as animal cells.

APPENDIX

Analysis of Net Potassium Flux into Neurospora According to a Three-Compartment Series Model Plots of total cell potassium vs. time for cells accumulating potassium show two distinct exponential components, as demonstrated in Figs. 1 and 2. The existence of two such components suggests that potassium enters two distinct compartments: a fixed charge region in the cell wall, and the intracellular space. It is likely (see p. 768) that the two compartments have independent access to potassium in the medium, and are thus arranged functionally in parallel (Fig. 10 *a*). But we cannot completely rule out the possibility of a series arrangement (Fig. 10 *b*), and need to compute the effect that such an arrangement would have on the apparent compartment sizes, rate constants, fluxes, and enzyme-kinetic constants which are eventually derived from data like those in Figs. 1 and 2.

Equations for the exchange of material in such series and parallel systems have been thoroughly described (44), and are presented here only to clarify the calculations which follow. We let X_0, X_1, and X_2 be the amount of potassium in the medium, in the fixed charge regions of the wall, and in the cytoplasm, respectively; and let k's be the first-order rate constants for transfer of potassium between compartments: k_{01}, for example, designating movement from medium to wall. Four assumptions are made for the sake of mathematical simplicity: (*a*) that the compartment arrangements are either purely series, or purely parallel; in Fig. 10 *a* there is no exchange k_{12}/k_{21}, and in Fig. 10 *b* there is no exchange k_{02}/k_{20}. (*b*) The initial values of X_1 and X_2 are zero; the total cell potassium in preincubated low K cells is only 7% of the normal value (see Table I). (*c*) The amount of potassium in the medium (X_0) is constant; this is assured by keeping the cell density in suspension low. (*d*) There is rapid mixing of potassium within any one compartment, so that the transfer rates at the boundaries are limiting.

Solutions to the differential equations for X_1 and X_2 may be written as follows:

$$\textit{Parallel case:}\quad X_1 = \frac{k_{01}}{k_{10}} X_0 \left(1 - e^{-k_{10}t}\right); \qquad X_2 = \frac{k_{02}}{k_{20}} X_0 \left(1 - e^{-k_{20}t}\right).$$

$$\textit{Series case:}\quad X_1 = \frac{k_{01}}{k_{10}} X_0 \left\{1 - \frac{1}{\lambda_1 - \lambda_2}\left[(\lambda_1 - k_{10})e^{-\lambda_1 t} - (\lambda_2 - k_{10})e^{-\lambda_1 t}\right]\right\} \qquad (6\,a)$$

$$X_2 = \frac{k_{12}}{k_{21}} \cdot \frac{k_{01}}{k_{10}} X_0 \left\{ 1 - \frac{1}{\lambda_1 - \lambda_2} [\lambda_1 e^{-\lambda_2 t} - \lambda_2 e^{-\lambda_1 t}] \right\} \qquad (6\ b)$$

where the graphically determined rate constants, λ_1 and λ_2, are given by

$$\frac{1}{2}(k_{10} + k_{12} + k_{21}) \pm \frac{1}{2}\sqrt{(k_{10} + k_{12} + k_{21})^2 - 4k_{10}k_{21}}.$$

The quantity $(X_1 + X_2)$ is measured, and for the parallel case graphic analysis of the type used in Fig. 2 gives directly the steady-state amounts of potassium in the wall ($X_{1\infty} = k_{01}X_0/k_{10}$) and the cytoplasm ($X_{2\infty} = k_{02}X_0/k_{20}$), as well as the rate constants (or time constants, $1/k$) for net movement of potassium into the wall (k_{10}) or cytoplasm (k_{20}). In the series case, however, neither the steady-state levels of potassium nor the compartmental rate constants relate simply to the graphic values. If C_1 and C_2 represent the steady-state quantities of potassium corresponding to λ_1 and λ_2, it can be shown that

$$k_{01}X_0 = \frac{d(X_1 + X_2)}{dt}\Big]_{t=0} = \lambda_1 C_1 + \lambda_2 C_2$$

$$k_{10} = \frac{\lambda_1^2 C_1 + \lambda_2^2 C_2}{k_{01}X_0} \qquad (7\ a)$$

$$k_{12} = \lambda_1\lambda_2 \left[\frac{C_1 + C_2}{k_{01}X_0} - \frac{1}{k_{10}} \right]$$

$$k_{21} = \frac{\lambda_1\lambda_2}{k_{10}} \qquad (7\ b)$$

$$X_{1\infty} = \frac{k_{01}X_0}{k_{10}} \qquad X_{2\infty} = \frac{k_{12}}{k_{21}} X_{1\infty} \qquad (8\ a, b)$$

This set of equations has been used to compute the values listed in columns 4–7 of Table V. Since there was no consistent dependence of λ_1 and λ_2 on the external potas-

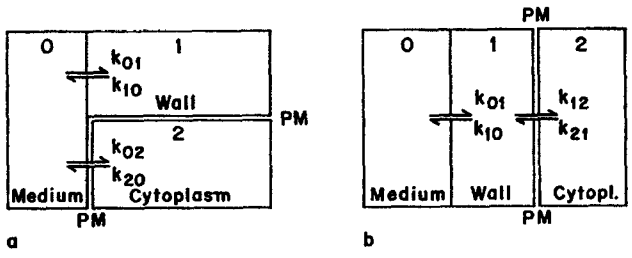

FIGURE 10. Diagrams of two possible compartmental arrangements of the cytoplasm and (fixed charge regions of) the cell wall of *Neurospora* in relation to the external medium. *a*, parallel; *b*, series. The medium, wall, and cytoplasm are designated as compartments 0, 1, and 2, respectively, and k_{01}, k_{20} . . . represent the rate constants for transfer of potassium from the medium to the wall, from the cytoplasm to the medium, etc. *PM* and the double lines designate the plasma membrane.

sium concentration, single average values were used in all the computations: $\lambda_1 = 0.833 \pm 0.067$ min^{-1}, and $\lambda_2 = 0.105 \pm 0.005$ min^{-1}. A comparison of the average value of k_{10} or k_{21} with λ_1 or λ_2 shows that simple graphic analysis would overestimate

TABLE V

COMPARTMENTAL PARAMETERS FOR POTASSIUM UPTAKE; SERIES CASE

Column No.	2	3	4	5	6	7	8	9	10
$[K]_o$	C_1	C_2	k_{10}	k_{21}	$X_{1\infty}$	$X_{2\infty}$	$C_1/X_{1\infty}$	$C_2/X_{2\infty}$	$k_{21}X_{2\infty}$
mM	*μmoles/g dry*		*min*$^{-1}$	*min*$^{-1}$	*μmoles/g dry*				*μmoles/g dry·min*
2.8	19.5	8.45	0.796	0.110	21.5	6.41	0.905	1.32	0.706
5.6	32.8	29.8	0.758	0.116	40.2	22.4	0.817	1.33	2.59
10.7	63.0	88.7	0.723	0.121	85.5	64.8	0.737	1.37	7.84
15	80.0	132.1	0.708	0.124	113.8	98.3	0.703	1.34	12.2
20	96.5	178.1	0.696	0.126	142.6	132.1	0.677	1.35	16.6
25	109.7	222.0	0.685	0.128	167.5	164.2	0.655	1.35	21.0
30	120.2	247.5	0.683	0.128	184.7	183.0	0.651	1.35	23.5
40	139.5	279.3	0.687	0.128	212.2	206.7	0.658	1.35	26.4
50	153.0	297.0	0.690	0.127	230.0	220.0	0.665	1.35	27.9
60	162.5	307.6	0.693	0.126	242.1	228.0	0.671	1.35	28.8
Averages			0.712	0.123			0.714	1.35	

C_1 and C_2 are the steady-state potassium levels associated with the two exponential components in the K uptake curves (e.g. Figs. 1 and 2), at each extracellular potassium concentration, $[K]_o$. The other symbols are defined in equations 7 *a,b* and 8 *a,b*, with respect to Fig. 10 *b*. The measured rate constants used were $\lambda_1 = 0.833$ and $\lambda_2 = 0.105$ min^{-1}.

TABLE VI

KINETIC CONSTANTS AND BINDING CONSTANTS COMPUTED FOR PARALLEL AND SERIES CASES

		Fast component (Cell wall)	Slow component (Cytoplasm)
Rate constants for net potassium uptake, *min*$^{-1}$	Parallel	0.833 ± 0.067	0.105 ± 0.005
	Series	0.712 ± 0.012	0.123 ± 0.002
Potassium concentration for half-maximal binding or net influx, *mM*	Parallel	32.0 ± 3.4	18.3 ± 0.3
	Series, $[K]_o$	38.3 ± 3.9	18.7 ± 0.3
	Series, $[K]_{wall}$	—	371 ± 10*
Maximal potassium bound, *μmoles/g dry*	Parallel	251 ± 30	—
	Series	408 ± 22	—
Maximal potassium influx, net, *mmoles/kg cell water·min*	Parallel	—	13.9 ± 0.2
	Series, $[K]_o$	—	12.6 ± 0.1
	Series, $[K]_{wall}$	—	18.4 ± 0.5

* This number should be multiplied by the activity coefficient of potassium within the fixed charge lattice. Diffusion studies on cation exchange resins (23) suggest a figure around 0.2, which is relatively independent of $[K]_o$ (at least in the range 0–60 mM).

the rate constant for net movement into the wall and underestimate that for net movement into the cytoplasm by 15–17%. Examination of $C_1/X_{1\infty}$ and $C_2/X_{2\infty}$ (columns 8 and 9, Table V) reveals that the simple analysis would also underestimate the net movement of potassium into the wall and overestimate that into the cytoplasm by about 30%.

A plot of $X_{1\infty}$ vs. $[K]_0$, however, still gives a rectangular hyperbola, similar to that in Fig. 5 ($B = X_{1\infty}$); but the least squares estimates of B_{max} and α become 408 ± 22 μmoles/g dry and 38.3 ± 3.9 mM, respectively.

The initial net flux into the cytoplasm must be zero, as shown by differentiation of equation 6 *b*. The rates needed—to compare with those plotted in Fig. 8—are those which would be obtained if the wall could be loaded with potassium instantly and then the wall and cytoplasm treated as a two-compartment system; i.e., $k_{21}X_{2\infty}$. These values are entered in the last column of Table V. When plotted against $[K]_o$, they again give a sigmoid curve similar to that in Fig. 8, having a maximal velocity of 32.0 ± 0.3 μmoles/g dry·min, or 12.6 ± 0.1 mmoles/kg cell water·min, and an apparent $K_{1/2}$ of 18.7 ± 0.3 mM. Neither value is significantly different from that obtained by assuming the parallel arrangement of wall and cytoplasm (see Table IV).

Obviously, the meaning of V_{max} and, particularly, $K_{1/2}$ will be altered if the active transport system has access only to the potassium concentration in the fixed charge regions of the wall. It could even be asked whether the whole form of the velocity equation might change, so that for example, a one-site pump operating on cell wall potassium might look like a two-site pump operating on potassium in the medium. This is not the case. The invariance of the equational form of the velocity curve can be demonstrated by substitution of $S = B = B_{max}[K]_o/(\alpha + [K]_o)$ into the Michaelis equation and into equation 1 or 2 above. The characteristics of the "real pump" in the series case can be obtained from a plot of $k_{21}X_{2\infty}$ vs. $X_{1\infty}$, fitted to equation 2: V_{max} = 46.8 ± 1.3 μmoles/g dry·min, or 18.4 ± 0.5 mmoles/kg cell water·min; $K_{\frac{1}{2}}$ = 188 ± 5 μmoles/g dry, or 371 ± 10 mM, using the conversion factors discussed in Methods. Table VI summarizes the various kinetic constants and binding constants obtained from the series case, in comparison with those obtained earlier for the assumed parallel arrangement of the cytoplasm and the fixed charge regions of the cell wall.

Early portions of this work were carried out in the Departments of Biology and Physiology at Western Reserve University, and were supported by Research Grant No. GB 6990 from the National Science Foundation and Public Health Service Research Grant No. GM 12790 from the National Institute of General Medical Sciences.

The remainder of the work, carried out at Yale University, was supported by Public Health Service Research Grants GM 15761 and GM 15858, and by a Public Health Service Research Career Development Award (No. GM 20163) to C. W. S., from the National Institute of General Medical Sciences.

The authors thank Mr. Robert Kopsack for expert technical assistance throughout the experiments, and Dr. W. K. Chandler for many helpful discussions.

Received for publication 3 November 1969.

REFERENCES

1. ARMSTRONG, W. McD., and A. ROTHSTEIN. 1964. Discrimination between alkali metal cations by yeast. I. Effect of pH on uptake. *J. Gen. Physiol.* **48**:61.

2. ARMSTRONG, W. McD., and A. ROTHSTEIN. 1967. Discrimination between alkali metal cations by yeast. II. Cation interactions in transport. *J. Gen. Physiol.* **50**:967.
3. BRIGGS, G. E., A. B. HOPE, and R. N. ROBERTSON. 1961. Electrolytes and Plant Cells.. Blackwell Scientific Publications Ltd., Oxford. 1–217.
4. CARPENTER, J. H. 1965. The Chesapeake Bay Institute technique for the Winkler dissolved oxygen method. *Limnol. Oceanogr.* **10**:141.
5. COHN, E. J., and J. T. EDSALL. 1943. Proteins, Amino Acids, and Peptides as Ion and Dipolar Ions. Reinhold Publishing Co., New York. 84.
6. Conway, E. J., and T. G. BRADY. 1950. Biological production of acid and alkali. 1. Quantitative relations of succinic and carbonic acids to the potassium and hydrogen ion exchange in fermenting yeast. *Biochem. J.* **47**:360.
7 CONWAY, E. J., P. F. DUGGAN, and R. P. KERNAN. 1963. Further studies on the nature of the physiological K-carrier in yeast. *Proc. Roy. Irish Acad. Sect. B. Biol. Geol. Chem. Sci.* **63**:93.
8. DAINTY, J., and A. B. HOPE. 1959. Ionic relations of the cells of *Chara australis*. I. Ion exchange in the cell wall. *Aust. J. Biol. Sci.* **12**:395.
9. DAINTY, J., A. B. HOPE, and C. DENBY. 1960. Ionic relations of cells of *Chara australis*. II. The indiffusible anions of the cell wall. *Aust. J. Biol. Sci.* **13**:267.
10. DAWSON, R. M. C., D. C. ELLIOTT, W. H. ELLIOTT, and K. M. JONES. 1959. Data for Biochemical Research. Oxford University Press, Oxford. 1–299.
11. DeTERRA, N., and E. L. TATUM. 1963. A relationship between cell wall structure and colonial growth in *Neurospora crassa*. *Amer. J. Bot.* **50**:669.
12. DIAMOND, J. M., and A. K. SOLOMON. 1959. Intracellular potassium compartments in *Nitella axillaris*. *J. Gen. Physiol.* **42**:1105.
13. DIXON, M., and E. C. WEBB. 1964. Enzymes. Academic Press, Inc., New York. 2nd edition. 54.
14. EBERHART, B. M. 1961. Exogenous enzymes of *Neurospora* conidia and mycelia. *J. Cell. Comp. Physiol.* **58**:11.
15. GALDIERO, F. 1968. Hydrogen ion binding of bacterial cell wall. *Experientia (Basel)*. **24**:352.
16. GOOD, N. E., G. D. WINGET, W. WINTER, T. N. CONNOLLY, S. IZAWA, and R. M. M. SINGH. 1966. Hydrogen ion buffers for biological research. *Biochemistry*. **5**:467.
17. GÜNTHER, T., and F. DORN. 1966. Über den K-Transport bei der K-Mangelmutante *E. coli* B 525. *Z. Naturforsch.* **21b**:1082.
18. HAROLD, F. M., and A. MILLER. 1961. Intracellular localization of inorganic polyphosphate in *Neurospora crassa*. *Biochim. Biophys. Acta*. **50**:261.
19. HELFFERICH, F. 1962. Ion Exchange. McGraw-Hill Book Co., New York. 1–624.
20. KEYNES, R. D. 1965. Some further observations on the sodium efflux in frog muscle. *J. Physiol. (London)*. **178**:305.
21. KEYNES, R. D., and R. C. SWAN. 1959. The effect of external sodium concentration on the sodium fluxes in frog skeletal muscle. *J. Physiol. (London)*. **147**:591.
22. KOTYK, A. 1962. Uptake of 2,4-dinitrophenol by the yeast cell. *Folia Microbiol.* **7**:109.
23 LAKSHMINARAYANAIAH, N. 1965. Transport phenomena in artificial membranes. *Chem. Rev.* **65**:491.
24. LESTER, G., D. STONE, and O. HECHTER. 1958. The effects of deoxycorticosterone and other steroids on *Neurospora crassa*. *Arch. Biochem. Biophys.* **75**:196.
25. LIVINGSTON, L. R. 1969. Locus-specific changes in cell wall composition characteristic of osmotic mutants of *Neurospora crassa*. *J. Bacteriol.* **99**:85.
26. MAHADEVAN, P. R., and E. L. TATUM. 1965. Relationship of the major constituents of the *Neurospora crassa* cell wall to wild-type and colonial morphology. *J. Bacteriol.* **90**:1073.
27. MANOCHA, M. S., and J. R. COLVIN. 1967. Structure and composition of the cell wall of *Neurospora crassa*. *J. Bacteriol.* **94**:202.
28. MARQUARDT, D. W. 1963. An algorithm for least-squares estimation of non-linear parameters. *J. Soc. Ind. Appl. Math.* **11**:431.
29. MATILE, P. 1964. Die Funktion proteolytischer Enzyme bei der Proteinaufnahme durch *Neurospora crassa*. *Naturwissenschaften*. **51**:489.

30. MONOD, J., J. WYMAN, and J. P. CHANGEUX. 1965. On the nature of allosteric transitions: a plausible model. *J. Mol. Biol.* **12**:88.
31. MULLINS, L. J., and A. S. FRUMENTO. 1963. The concentration dependence of sodium efflux from muscle. *J. Gen. Physiol.* **46**:629.
32. POST, R. L., and P. C. JOLLY. 1957. The linkage of sodium, potassium, and ammonium active transport across the human erythrocyte membrane. *Biochim. Biophys. Acta.* **25**:118.
33. PRESSMAN, B. C. 1967. Biological applications of ion-specific glass electrodes. *In* Methods in Enzymology. R. W. Estabrook and M. E. Pullman, editors. Academic Press, Inc., New York. **10**:714.
34. ROTHSTEIN, A., and A. D. HAYES. 1956. The relationship of the cell surface to metabolism. XIII. The cation-binding properties of the yeast cell surface. *Arch. Biochem. Biophys.* **63**:87.
35. SACHS, J. R. 1967. Competitive effects of some cations on active potassium transport in the human red blood cell. *J. Clin. Invest.* **46**:1433.
36. SACHS, J. R , and L. G. WELT. 1967. The concentration dependence of active potassium transport in the human red blood cell. *J. Clin. Invest.* **46**:65.
37. SCATCHARD, G. 1949. The attractions of proteins for small molecules and ions. *Ann. N.Y. Acad. Sci.* **51**:660.
38. SCHAEDLE, M., and L. JACOBSON. 1965. Ion absorption and retention by *Chlorella pyrenoidosa*. I. Absorption of potassium. *Plant Physiol.* **40**:214.
39. SHATKIN, A. J., and E. L. TATUM 1959. Electron microscopy of *Neurospora crassa* mycelia. *J. Biophys. Biochem. Cytol.* **6**:423.
40. SLAYMAN, C. L., and C. W. SLAYMAN. 1968. Net uptake of potassium in *Neurospora*. Exchange for sodium and hydrogen ions. *J. Gen. Physiol.* **52**:424.
41. SLAYMAN, C. W., and E. L. TATUM. 1964. Potassium transport in *Neurospora*. I. Intracellular sodium and potassium concentrations, and cation requirements for growth. *Biochim. Biophys. Acta* **88**:578.
42. SLAYMAN, C. W., and E. L. TATUM. 1965. Potassium transport in *Neurospora*. II. Measurement of steady-state potassium fluxes. *Biochim. Biophys. Acta.* **102**:149.
43. SLAYMAN, C. W., and E. L. TATUM. 1965. Potassium transport in *Neurospora*. III. Isolation of a transport mutant. *Biochim. Biophys. Acta.* **109**:184.
44. SOLOMON, A. K. 1960. Compartmental methods of kinetic analysis. *In* Mineral Metabolism. C. L. Comar and F. Bronner, editors. Academic Press, Inc., New York. 1 (Pt.A): 119.
45. TANFORD, C. 1962. The interpretation of hydrogen ion titration curves of proteins. *Advan. Protein Chem.* **17**:69.
46. TREVITHICK, J. R., and R. L. METZENBERG. 1966. Genetic alteration of pore size and other properties of the Neurospora cell wall. *J. Bacteriol.* **92**:1016.
47. UMBREIT, W. W., R. H. BURRIS, and J. F. STAUFFER. 1964. Manometric Techniques. Burgess Publishing Co., Minneapolis, Minn. 4th edition. 1–305.
48. WEAST, R. C., S. M. SELBY, and C. D. HODGMAN. 1965. Handbook of Chemistry and Physics. Chemical Rubber Co , Cleveland, Ohio 46th edition. D-78 and D-79.
49. WYMAN, J. 1967. Allosteric linkage. *J. Amer. Chem. Soc.* **89**:2202.